THE ARCHIVE OF MECHANICAL ENGINEERING

VOL. LIV 2007 Number 4

DOI: 10.24425/ame.2007.131563

Key words: parallel mechanism, pose estimation, wire sensor, collisions-free workspace, Jacobian matrix

MARTA GÓRA [*], *JÓZEF KNAPCZYK*[*], *MICHAŁ MANIOWSKI*[**]

ESTIMATION OF PLATFORM SPATIAL POSE AND DISPLACEMENT OF PARALLEL MECHANISM USING WIRE-BASED SENSORS

This paper presents an estimation method for the spatial pose and displacement parameters of multi-rod suspension mechanism, based on measurement results by using wire sensors. Some changes of position and orientation of the platform fixed to wheel knuckle cause corresponding changes of sensors' cable lengths. The fixation points of the cable sensors are selected with the collision-free conditions taken into account. Numerical example deals with platform poses and positioning of the sensors that satisfy the measurement conditions.

NOMENCLATURE

$\boldsymbol{R}$ – orientation matrix;
$\boldsymbol{a}_i$ – position vector of point A_i with respect to coordinate system $Oxyz$;
$\boldsymbol{b}_i$ – position vector of point B_i with respect to coordinate system $Oxyz$;
$\boldsymbol{o}$ – position vector of original point (O) of reference system;
$\boldsymbol{l}_i$ – link vector of i-th leg/cable (with length l_i);
$\hat{\boldsymbol{e}}$ – unit vector;
$\widehat{\boldsymbol{e}}$ – spatial vector;
$\times$ – cross vector product;
$\circ$ – dot vector product.

1. Introduction

There are some advantages of utilizing cable-based parallel mechanisms, for example minimum moving inertia and large range of motion. Cable-

[*] *Cracow University of Technology, Institute of Automobiles and Combustion Engines, Al. Jana Pawła II 37b, 31-864 Kraków, Poland; E-mail: j_kn@mech.pk.edu.pl*

[**] *Cracow University of Technology, Institute of Rail Vehicles, Al. Jana Pawła II 37b, 31-864 Kraków, Poland; E-mail: maniowski@m8.mech.pk.edu.pl*

guided parallel mechanisms are used in manufacturing industry and in the construction industry as positioning mechanisms or handling mechanisms, for example in special cranes. The moving platform is guided by the attached cables that are connected to the base. Originally, these mechanisms were used in the docks for ship building and loading works [6]. New applications of the tendon-based Stewart platforms need new method for analysis of the workspace in order to completely control all degrees of freedom and reduce or eliminate singularities or collisions, and to obtain the desired stiffness distribution [10].

Jeong et al. [6] developed a parallel wire mechanism with six wires for pose measurement purposes. The pose of the end-effector was calculated using the wire lengths obtained from corresponding encoders. The forward position problem was solved numerically. The reported accuracy was about 0.05 mm and 0.1 deg for translation and orientation respectively.

Table 1.

Systematization of spatial mechanism with platform consisting of rigid links and cables

Type	Rigid links	Cables		Remarks
		Loaded	Unloaded	
I	+	-	-	Typical Stewart Platform [8, 9].
II	+	-	+	Measured cable lengths used to simplify solution of the mechanism position problem [6] or to estimate the end-effector pose and displacement.
III	+	+	-	Hybrid type, e.g. model of knee joint [5], where bones are modeled as rigid bodies, and ligaments as cables.
IV	-	+	-	Platform with cables spatially situated or with force closure, e.g. by using gravity force [1, 9, 10].

Table 1 presents the systematization of spatial parallel mechanisms with rigid links and cables. In the case when moving platform performs some work (type III and IV) by load action along a given trajectory, the workspace limitations result from conditions of cable tensions [5], [9]. The cable lengths (type II) can be used to simplify the solution of the direct position problem of the end-effector of the considered spatial mechanism.

The measurement system, presented in Fig.1a, [2], consists of two planar platforms linked by cables, where moving platform B is attached to the end-effector, and the second platform is fixed to the base. The variable distances between corresponding points of the two platforms are measured by using wire sensors. In each wire sensor, a pulley with spiral spring is attached to the base platform A, Fig. 1b. The wires are unloaded and their tensions result

from the spring preload force in the range of a few [N]. The resulting load from tension forces of wires usually does not influence the load distribution in the mechanism. The considered mechanism is of II type from Table 1. The displacement of the end-effector attached to moving platform with respect to the base platform causes the changes of the wire lengths which are measured by using encoders. It is possible to determine the position and orientation of the end-effector [3] by solving the direct position problem formulated for the mechanism with platform of six DOF by using the wire lengths and the coordinates of respective platform points [4], [8].

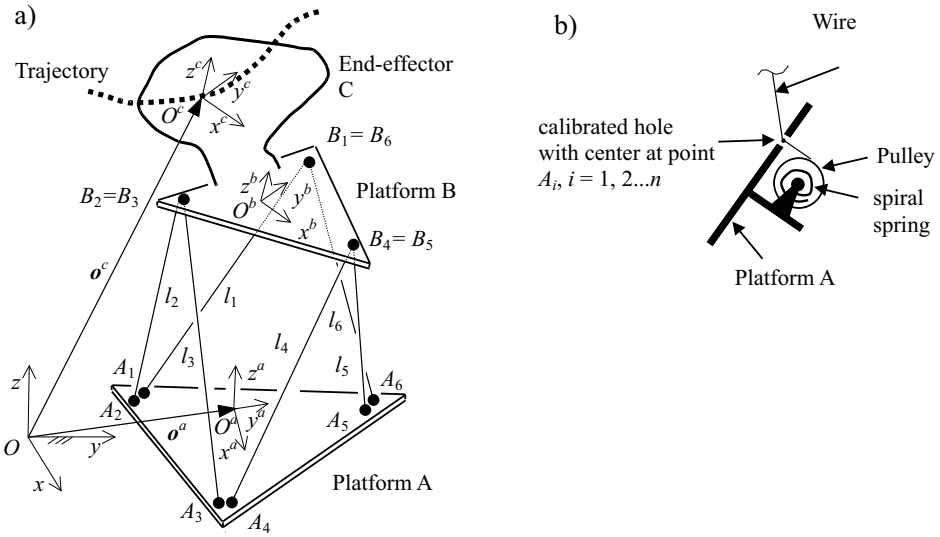

Fig. 1. a) Kinematic scheme of platform system with wire sensors; b) Scheme of wire sensor

The presented system can be used to measure some small displacements caused by dynamic excitations in low frequency range. The algorithm for solving the forward position problem for the considered measurement system is proposed in this paper (Fig. 1a). The collision-free conditions for the wire are determined taking into account the work space limitations and the allowed changes of the wire lengths. The conditioning and accuracy analysis of the measurement system are presented in [2].

2. Solution of forward position problem

The end-effector spatial positions and displacements are determined on the basis of p poses described by position vectors ($\boldsymbol{o}_j^c$) and orientation matrices ($\boldsymbol{R}_j^c$), for $j = 1, 2...p$. Unknown poses of the end-effector can be computed using known poses of the measuring platform B with respect to base platform

A, where the measuring platform (B, Fig. 1a) is fixed to the end-effector (C, Fig. 1a). The measuring platforms are assumed to be planar, what simplifies building prototypes, their dimensioning, and solving the forward position problem.

Additional assumptions for the measuring mechanism model are the following:

a) the platforms are rigid, the cables are inextensible, and the joints are ideal;
b) the measuring mechanism pose is distant from singularity;
c) the cables are always in tension, not interfering with other cables or environment;
d) the parallel structure is dimensioned to resemble a regular octahedron, what reduces number of the mechanism configurations, and simplifies solution of the forward position problem [3].

In order to determine the measuring platform pose, the following data should be given:

a) constant coordinates of the points on the platforms A_i and B_i ($\boldsymbol{a}_i$; $\boldsymbol{b}_i^b$; $i = 1, 2...n$);
b) variable lengths of all the cables/legs ($l_i = \|\boldsymbol{l}_i\|$; $\boldsymbol{l}_i = \boldsymbol{b}_i - \boldsymbol{a}_i$; $i = 1, 2...n$).

The i-th cable vector $\boldsymbol{l}_i$ is expressed by a function of three orientation parameters ($\boldsymbol{R}^{ba}$), and three components of the position vector ($\boldsymbol{o}^{ba}$) of platform B with respect to platform A, in the following manner [2], [4]:

$$\boldsymbol{l}_i = \boldsymbol{R}^{ba}\boldsymbol{b}_i^b + \boldsymbol{o}^{ba} - \boldsymbol{a}_i; \qquad i = 1, 2...n; \qquad n \geqslant 6 \tag{1}$$

where:
$\boldsymbol{b}_i^b$ – position vector of the point Bi in reference system fixed to platform B,
$\boldsymbol{o}^{ba}$ – position vector of the point O^b in reference system of the platform A.
Position problem of the considered parallel mechanism is based on a solution of a set of constraints equations, which can be expressed by constant distance between the corresponding points of two platforms:

$$\boldsymbol{l}_i^T \ \boldsymbol{l}_i = l_i^2; \qquad i = 1, \ 2... \ n; \qquad n \geqslant 6 \tag{2}$$

The vector method is used to formulate the constraint equations [5]. Three tetrahedrons ($A_1A_3A_6B_1$, $A_4A_5B_4B_6$, and $A_3B_2B_1B_4$) are selected in the mechanism scheme in Fig. 2. The following unit vectors $\hat{\boldsymbol{l}}_1$, $\hat{\boldsymbol{l}}_4$, and $\hat{\boldsymbol{b}}_12$ are determined by using the three vector equation [9]:

$$\hat{\boldsymbol{e}}_k = \frac{[((\hat{\boldsymbol{e}}_i \circ \hat{\boldsymbol{e}}_k) - (\hat{\boldsymbol{e}}_i \circ \hat{\boldsymbol{e}}_j)(\hat{\boldsymbol{e}}_j \circ \hat{\boldsymbol{e}}_k))\hat{\boldsymbol{e}}_i + ((\hat{\boldsymbol{e}}_j \circ \hat{\boldsymbol{e}}_k) - (\hat{\boldsymbol{e}}_i \circ \hat{\boldsymbol{e}}_j)(\hat{\boldsymbol{e}}_i \circ \hat{\boldsymbol{e}}_k))\hat{\boldsymbol{e}}_j + p_k\sqrt{D_k}(\hat{\boldsymbol{e}}_i \times \hat{\boldsymbol{e}}_j)}{1 - (\hat{\boldsymbol{e}}_i \circ \hat{\boldsymbol{e}}_j)^2} \tag{3}$$

where:
$D_k = 1 - (\hat{\boldsymbol{e}}_i \circ \hat{\boldsymbol{e}}_j)^2 - (\hat{\boldsymbol{e}}_i \circ \hat{\boldsymbol{e}}_k)^2 - (\hat{\boldsymbol{e}}_j \circ \hat{\boldsymbol{e}}_k)^2 + 2(\hat{\boldsymbol{e}}_i \circ \hat{\boldsymbol{e}}_j)(\hat{\boldsymbol{e}}_i \circ \hat{\boldsymbol{e}}_k)(\hat{\boldsymbol{e}}_j \circ \hat{\boldsymbol{e}}_k)$;
$p_k = \pm 1$, depends on the tetrahedron configuration; $i, j, k = 1, 2...6$.

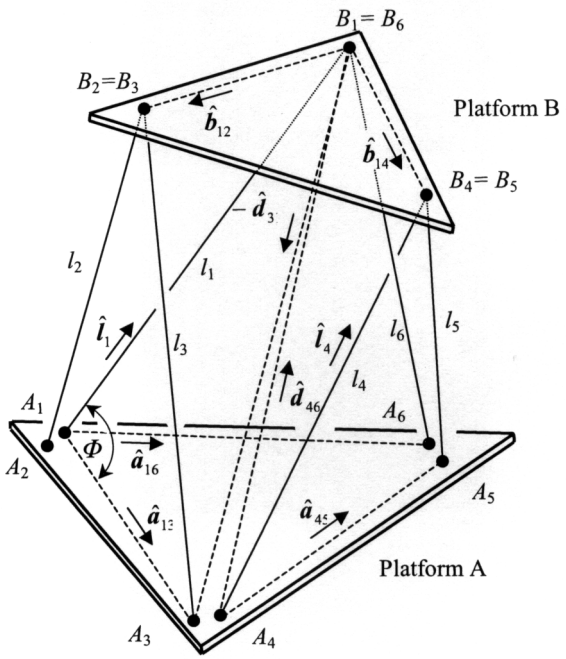

Fig. 2. Scheme of platform mechanism with cables for measurement of spatial pose and displacement of end-effector

Coordinates of platform B points are determined in successive steps (Tab.1) dependent on an auxiliary variable, defined as an angle between the unit vectors $\hat{\boldsymbol{a}}_{13}$ and $\hat{\boldsymbol{d}}_1$ (Fig. 2).

The constraint equations (2) are solved using an iterative algorithm (Newton-Gauss [9]). The platform position and orientation are computed on the basis of the presented algorithm (angle Φ and vectors $\boldsymbol{b}_1$, $\boldsymbol{b}_4$, and $\boldsymbol{b}_3$).

The position of platform B is described by origin ($\boldsymbol{o}^b$) of the reference system $\{O^b x^b y^b z^b\}$ with respect to the fixed reference system $\{Oxyz\}$. The origin ($\boldsymbol{o}^b$) is placed at the center of area of the planar platform B, i.e. for an equilateral triangle, according to the following formula:

$$\boldsymbol{o}^b = (\boldsymbol{b}_1 + \boldsymbol{b}_2 + \boldsymbol{b}_4)/3 \tag{4}$$

Orientation of platform B can be determined using three orientation angles. A few conventions of this approach are known [9]. Roll-pitch-yaw convention is used usually in vehicle dynamics for vehicle body orientation [3], [4], [7].

Table 2.

Solution stages of the forward position problem

Stage	$\hat{\boldsymbol{e}}_i$	$\hat{\boldsymbol{e}}_j$	$\hat{\boldsymbol{e}}_k$	Position vector of platform B points
1	$\hat{\boldsymbol{a}}_{16}$	$\hat{\boldsymbol{a}}_{13}$	$\hat{\boldsymbol{l}}_1$	$\boldsymbol{b}_1 = \boldsymbol{a}_1 + l_1\hat{\boldsymbol{l}}_1$
2	$\hat{\boldsymbol{a}}_{45}$	$\hat{\boldsymbol{d}}_{46}$	$\hat{\boldsymbol{l}}_4$	$\boldsymbol{b}_4 = \boldsymbol{a}_4 + l_4\hat{\boldsymbol{l}}_4$
3	$\hat{\boldsymbol{b}}_{14}$	$-\hat{\boldsymbol{d}}_{31}$	$\hat{\boldsymbol{b}}_{12}$	$\boldsymbol{b}_3 = \boldsymbol{b}_1 + b_{12}\hat{\boldsymbol{b}}_{12}$
where: $\boldsymbol{a}_{ij} = \boldsymbol{a}_j - \boldsymbol{a}_i$; $\boldsymbol{b}_{ij} = \boldsymbol{b}_j - \boldsymbol{b}_i$; $\boldsymbol{d}_{ij} = \boldsymbol{b}_j - \boldsymbol{a}_i$; $\hat{\boldsymbol{a}}_{ij} = \boldsymbol{a}_{ij}/a_{ij}$; $\hat{\boldsymbol{b}}_{ij} = \boldsymbol{b}_{ij}/b_{ij}$; $\hat{\boldsymbol{d}}_{ij} = \boldsymbol{d}_{ij}/d_{ij}$.				

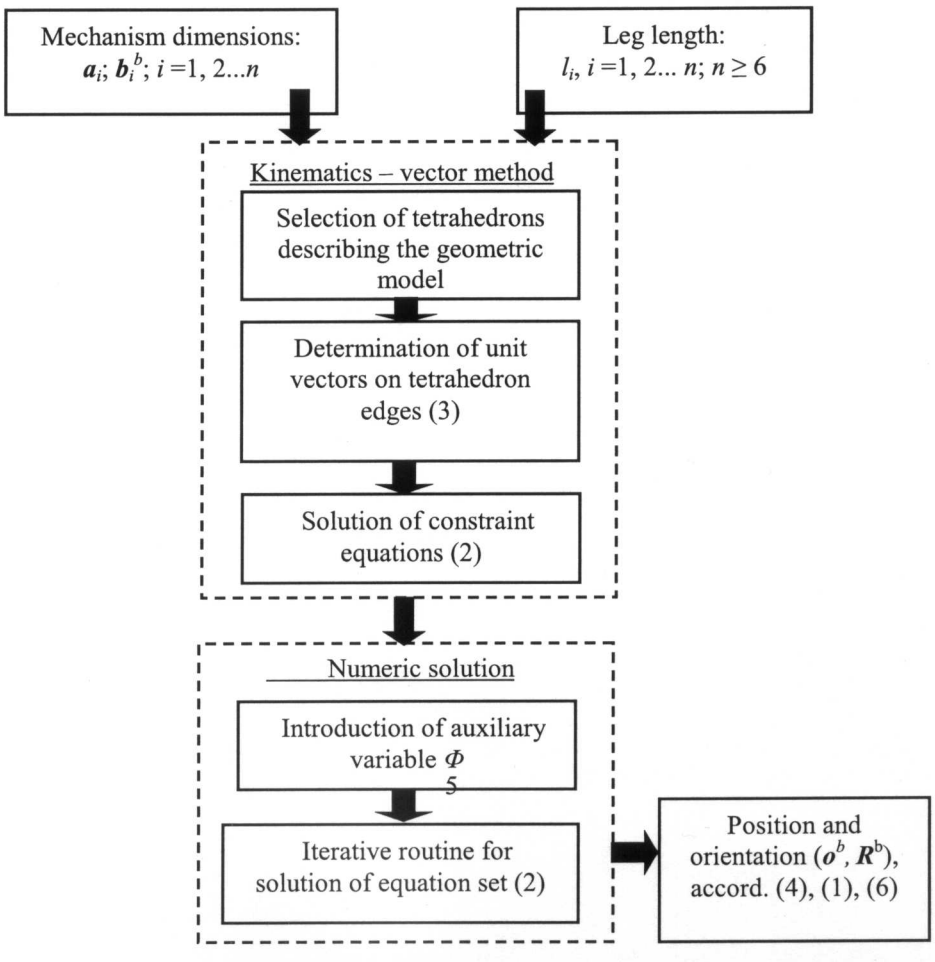

Fig. 3. Block diagram for solution of forward position problem for platform mechanism

The orientation matrix is composed of three elementary rotations about axes of fixed reference system, in the following sequence: (I) rotation about

x-axis with ϕ – roll angle, (II) rotation about y-axis with θ – pitch angle, and (III) rotation about z-axis with ψ – yaw angle, where the rotation senses are in accordance with the right-hand rule. The sequence of rotations is written down as a matrix multiplication as follows:

$$\boldsymbol{R}^b(\phi,\ \theta,\ \psi) = \boldsymbol{R}^b_z(\psi)\ \boldsymbol{R}^b_y(\theta)\ \boldsymbol{R}^b_x(\phi) \tag{5}$$

When the three orientation angles (φ, θ, ψ) of platform B are given, the orientation matrix can be determined using the following formula [7]:

$$\boldsymbol{R}^b(\phi,\ \theta,\ \psi) = \begin{bmatrix} c\psi c\theta & c\psi s\theta s\phi - s\psi c\phi & c\psi s\theta c\phi + s\psi s\phi \\ s\psi c\theta & s\psi s\theta s\phi + c\psi c\phi & s\psi s\theta c\phi - c\psi s\phi \\ -s\theta & c\theta s\phi & c\theta c\phi \end{bmatrix} \tag{6}$$

Inverse problem of finding the three angles for the given orientation matrix can be solved using the well known relationships [9]. The following stages of the forward position problem of the platform mechanism are described by the block diagram presented in Fig. 3.

3. Cable interference and collisions with environment

Reading of the measuring cables length is correct only when the cables are in tension and without collisions. It is assumed that length of each measuring cable is bounded by:

$$l_{i,\min} < l_i < l_{i,\max};\quad i = 1,\ 2...n;\quad n \geqslant 6 \tag{7}$$

In the case of violation of the lower bound (7), the cable drum can not wind-up more cable and sustain its tension. In the case of violation of the upper bound (7), the cable drum is fully unwound, i.e. the cable has reached its maximal length.

The measuring cable (Fig. 4) can be modeled by a cylindrical surface with known radius (r_i) and axis described by parametric equation (Eq. 8) of line in space:

$$\boldsymbol{q}_{ik} = \boldsymbol{a}_i + \boldsymbol{l}_i t_k,\quad t_k \in R,\quad k \in N^+ \tag{8}$$

where:
$\boldsymbol{q}_{ik}$ – position vector of k-th point (Q_{ik}) lying on the line l_i as function of parameter t_k;
$\boldsymbol{l}_i$ – direction vector of the cylinder axis.

In order to avoid interference between the cables (collisions of the cables) during measurements of the end-effector displacement, the distances between each couple (i and j) of the cables are determined using the following formula:

$$h_{ij} = d_{ij} - (r_i + r_j); \quad i, j = 1, 2...n; \quad n \geqslant 6; \quad i \neq j \tag{9}$$

where: d_{ij} – distance between the skew lines, expressed by:

$$d_{ij} = \frac{\left|\left[\boldsymbol{l}_i, \boldsymbol{l}_j, \boldsymbol{a}_j - \boldsymbol{a}_i\right]\right|}{\left|\boldsymbol{l}_i \times \boldsymbol{l}_j\right|} \tag{10}$$

Two cables (i-th and j-th) are in collision when the following condition is not fulfilled:

$$h_{ij} > 0; \quad i, j = 1, 2...n; \quad n \geqslant 6; \quad i \neq j \tag{11}$$

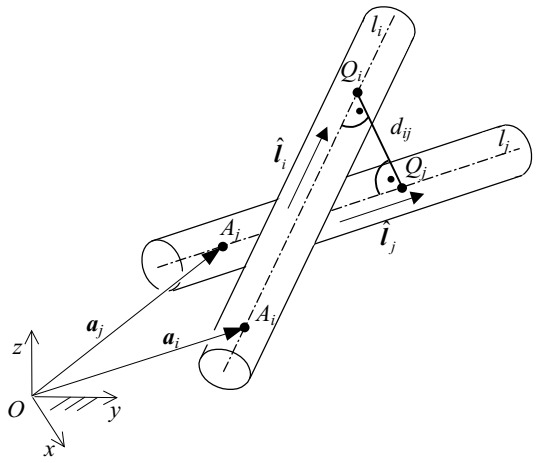

Fig. 4. Cables of measuring system (l_i and l_j) modeled by cylinders in space

Condition (11) does not concern cables having one common origin in the platform joints ($i = 2$, $j = 3$; $i = 4$, $j = 5$; $i = 1$, $j = 6$). In other cases, when the condition (11) is not fulfilled, the location of the cylinder intersection point should be checked. If the location is between the platform A and B, then the real contact (collision) of the cylinders takes place.

Determination of the cables intersection point, first method

The intersection point for two axes of cylinders is determined by using the formula describing the distance between a point and the axis of cylinder, taking into account its radius:

$$\frac{\left\|(\boldsymbol{q}_j - \boldsymbol{a}_i) \times \boldsymbol{l}_i\right\|}{l_i} - (r_i + r_j) = 0 \tag{12}$$

On the basis of formula (8) and (12) we derive a second order polynomial equation with t_k as unknown:

$$Kt_k^2 + Nt_k + P = 0 \tag{13}$$

where:
$K = K_{yz} + K_{xz} + K_{xy}$,
$N = N_{yz} + N_{xz} + N_{xy}$,
$P = P_{yz} + P_{xz} + P_{xy} - (r_i + r_j)^2 l_i^2$,
$K_{no} = l_{jn}^2 l_{io}^2 - 2l_{jn}l_{jo}l_{in}l_{io} + l_{jo}^2 l_{in}^2$,
$N_{no} = 2a_{jn}l_{jn}l_{io}^2 - 2a_{in}l_{jn}l_{io}^2 - 2a_{jn}l_{jo}l_{io}l_{in} - 2a_{jo}l_{jn}l_{io}l_{in} + 2a_{io}l_{jn}l_{io}l_{in} + 2a_{in}l_{jo}l_{io}l_{in} + 2a_{jo}l_{jo}l_{in}^2 - 2a_{io}l_{jo}l_{in}^2$,
$P_{no} = a_{jn}^2 l_{io}^2 - 2a_{in}a_{jn}l_{io}^2 + a_{in}^2 l_{io}^2 - 2a_{jn}a_{jo}l_{io}l_{in} + 2a_{io}a_{jn}l_{io}l_{in} + 2a_{in}a_{jo}l_{io}l_{in} - 2a_{in}a_{io}l_{io}l_{in} + a_{jo}^2 l_{in}^2 - 2a_{jo}a_{io}l_{in}^2 + a_{io}^2 l_{in}^2$,
for $n, o = x, y, z$.
The cables collision takes place when at least one of the equation (13) solution belongs to the range $t_k \in [0, 1]$, where for $t_k = 0$, $\boldsymbol{q}_j = \boldsymbol{a}_j$ (platform A), and for $t_k = 1$, $\boldsymbol{q}_j = \boldsymbol{b}_j$ (platform B).

Determination of cable intersection point, second method

The longitudinal axis of i-th and j-th leg (cable) of the mechanism (Fig. 4) can be described using the equations:

$$\boldsymbol{q}_{ik} = \boldsymbol{a}_i + \boldsymbol{l}_i\, t_k; \qquad t_k \in R; \qquad k \in N^+ \tag{14}$$

$$\boldsymbol{q}_{jk} = \boldsymbol{a}_j + \boldsymbol{l}_j\, s_m; \qquad s_m \in R; \qquad m \in N^+ \tag{15}$$

where:
$\boldsymbol{q}_{ik}$ – position vector of k-th point belonged to axis l_i as function of parameter t_k;
$\boldsymbol{q}_{jm}$ – position vector of m-th point belonged to axis l_j as function of parameter s_m.

The conditions for a common perpendicular to the axes l_i and l_j are as follows:

$$(\boldsymbol{q}_{jm} - \boldsymbol{q}_{ik})^T \boldsymbol{l}_i = 0 \tag{16}$$

$$(\boldsymbol{q}_{jm} - \boldsymbol{q}_{ik})^T \boldsymbol{l}_j = 0 \tag{17}$$

Using formulas (14) and (15) for (16) and (17), we derive the matrix equation:

$$\begin{bmatrix} s_m \\ t_k \end{bmatrix} = \begin{bmatrix} p_{11} & p_{12} \\ p_{21} & p_{22} \end{bmatrix}^{-1} \begin{bmatrix} w_1 \\ w_2 \end{bmatrix} \tag{18}$$

where: $p_{11} = \boldsymbol{l}_i^T \boldsymbol{l}_j$; $p_{12} = p_{11}$; $p_{21} = l_j^2$; $p_{22} = -l_i^2$; $w_1 = \boldsymbol{l}_i^T(\boldsymbol{a}_i - \boldsymbol{a}_j)$; $w_2 = \boldsymbol{l}_j^T(\boldsymbol{a}_i - \boldsymbol{a}_j)$.

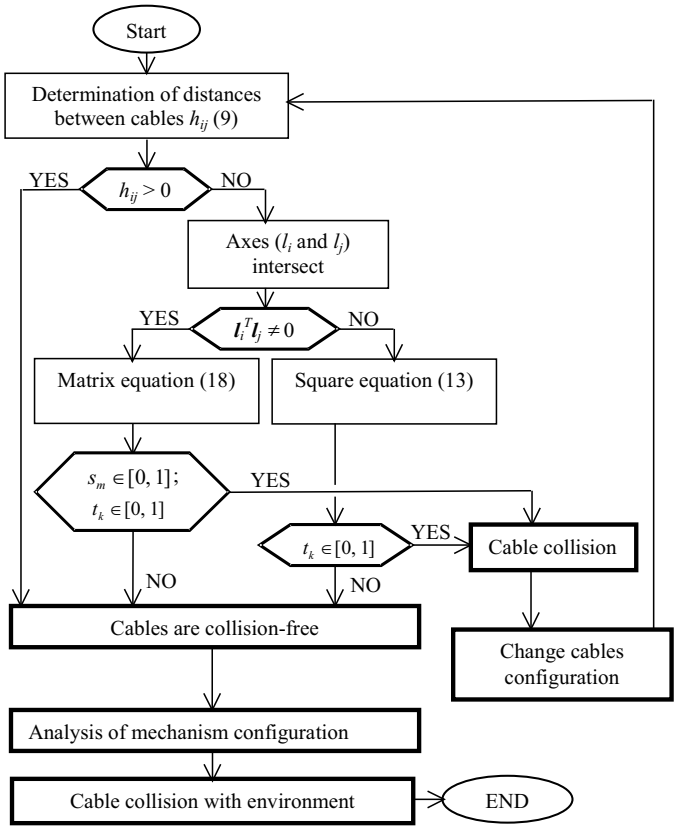

Fig. 5. Block scheme of verification procedure for collision-free condition of cables

The square matrix in equation (18) can be inverted under the condition $\boldsymbol{l}_i^T \boldsymbol{l}_j \neq 0$, what means that two vectors $\boldsymbol{l}_i$ and $\boldsymbol{l}_j$ are not perpendicular. When

anyone among solutions of equation (18) belongs to the range $t_k \in [0,1]$, $s_m \in [0,1]$ (where for $t_k = 0$, $\boldsymbol{q}_j = \boldsymbol{a}_j$, for $t_k = 1$, $\boldsymbol{q}_j = \boldsymbol{b}_j$, for $s_m = 0$, $\boldsymbol{q}_j = \boldsymbol{a}_j$, and for $s_m = 1$, $\boldsymbol{q}_j = \boldsymbol{b}_j$), then the cables collision takes place.

The problem for the cable collision with environment is formulated using the cylinders for description of the suspension rods, and the planes for description of the platforms and other surfaces. The positions of two cylinders are determined according to the block scheme presented in Fig. 5.

The collision of a cylinder with a plane can be detected by finding the intersection point of the plane with the cylinder axis displaced by the cylinder radius (r_i). If the plane intersects with this axis, then the condition that the intersection point belongs to the plane is verified. If the directional vector of the plane (describing an environment object) is perpendicular to the cylinder axis (cable) and this axis does not lie in the plane, then the cable does not collide with the environment.

4. Analysis of mechanism configuration

The considered mechanism should not change its configuration in the given workspace of the measurements. In order to verify this condition some features of the mechanism Jacobian matrix ($\boldsymbol{J}$) can be used. When the Jacobian matrix determinant ($det(\boldsymbol{J})$) is different from zero in any point of the workspace, then the considered mechanism is singularity-free [10], [11].

Differentiating the constraint equations (2) with respect to time and assuming that length of any leg can change, we can write the linear relationship between the end-effector velocity state ($\boldsymbol{v}_0^c$ – velocity vector of point O and $\boldsymbol{\omega}^c$ – platform angular velocity) and differential changes of the leg lengths ($\dot{\boldsymbol{l}}$) in the form:

$$\dot{\boldsymbol{l}} = \boldsymbol{J}\hat{\boldsymbol{v}}^c \tag{19}$$

where:
$\dot{\boldsymbol{l}} = [\dot{l}_1 \dot{l}_2 \ldots \dot{l}_n]^T$; $\hat{\boldsymbol{v}}^c = [[\boldsymbol{v}_0^c]^T [\boldsymbol{\omega}^c]^T]^T$; $n \geq 6$,
$\hat{\boldsymbol{v}}^c$ – space vector of the end-effector, $\boldsymbol{J}$ – Jacobian matrix.

Equation (19) describes the inverse kinematic problem (first order) for the mechanism with parallel structure [2]. The Jacobian matrix, dependent on the mechanism configuration, can be defined as:

$$\boldsymbol{J}_{n\times 6} = [\hat{\boldsymbol{l}}_1 \hat{\boldsymbol{l}}_2 \ldots \hat{\boldsymbol{l}}_n]^T \tag{20}$$

where: $\hat{\boldsymbol{l}}_i = [\hat{\boldsymbol{l}}_i^T ((\boldsymbol{o}^c - \boldsymbol{b}_i) \times \hat{\boldsymbol{l}}_i)^T]^T$; $\hat{\boldsymbol{l}}_i$ – unit vector of i-th leg/cable.

When the considered mechanism with six legs (i = 1 do 6) is in nonsingular configuration, the direct kinematic problem can be formulated:

$$\boldsymbol{H}\dot{\boldsymbol{l}} = \hat{\boldsymbol{v}}^c \tag{21}$$

where: $\boldsymbol{H}\boldsymbol{J} = \boldsymbol{I}$.

The specific properties of the mechanism can be analyzed by using a condition number of Jacobian matrix ($\chi(\boldsymbol{J})$) [2], [11], defined as the ratio of the largest (σ_{max}) to the smallest (σ_{min}) singular value of the matrix $\boldsymbol{J}$ [11]:

$$\chi(\boldsymbol{J}) = \frac{\sigma_{max}}{\sigma_{min}} \tag{22}$$

The condition number of the Jacobian matrix depends on the leg lengths and mechanism configurations. Those points in the workspace where condition number (22) is equal to 1 are called isotropic points. In these points of the workspace the considered mechanism is characterized by the most direct transmission ratio between the platform displacement and the length changes of the linear actuators. In this case, the Jacobian matrix of the mechanism satisfies the isotropic condition ($\boldsymbol{J}^T\boldsymbol{J} = \tau^2\boldsymbol{I}$, τ – scalar). When the condition number $\chi(\boldsymbol{J})$ approaches infinity, the matrix is said to be ill-conditioned, this means that the mechanism approaches a singularity.

5. Numerical examples

The presented example deals with the parallel mechanism with cables (Fig. 1) adapted to the so-called elastokinematical measurements of the wheel guiding mechanism used in automobiles, Fig. 6. The measurements are used to determine some changes in the position and orientation of the wheel carrier with respect to the car body, caused be the changes of the wheel load during a selected maneuver.

Platform B is fixed to the wheel carrier (treated as the end-effector with a local reference system positioned at the wheel center), and the base platform A is fixed to the car body, Fig. 6. The cables are located between the suspension rods, Fig. 6b. The wires layout and the position of the platform A, adjusted for the actual suspension mechanism, are shown in Fig. 7.

In order to verify the computer program for determination of the position and displacement of the cable mechanism, some numerical examples are solved. The rigidity condition for the cables is introduced. We can obtain the platform displacements, neglecting the end-effector as an active element, by assuming the respective lengths of the selected cables (l_i = var, i = 3, 5; l_i = const., i = 1, 2, 4, 6). The input data for the direct position problem

describing the coordinates of platform points and the lengths of cables are presented in Table 3.

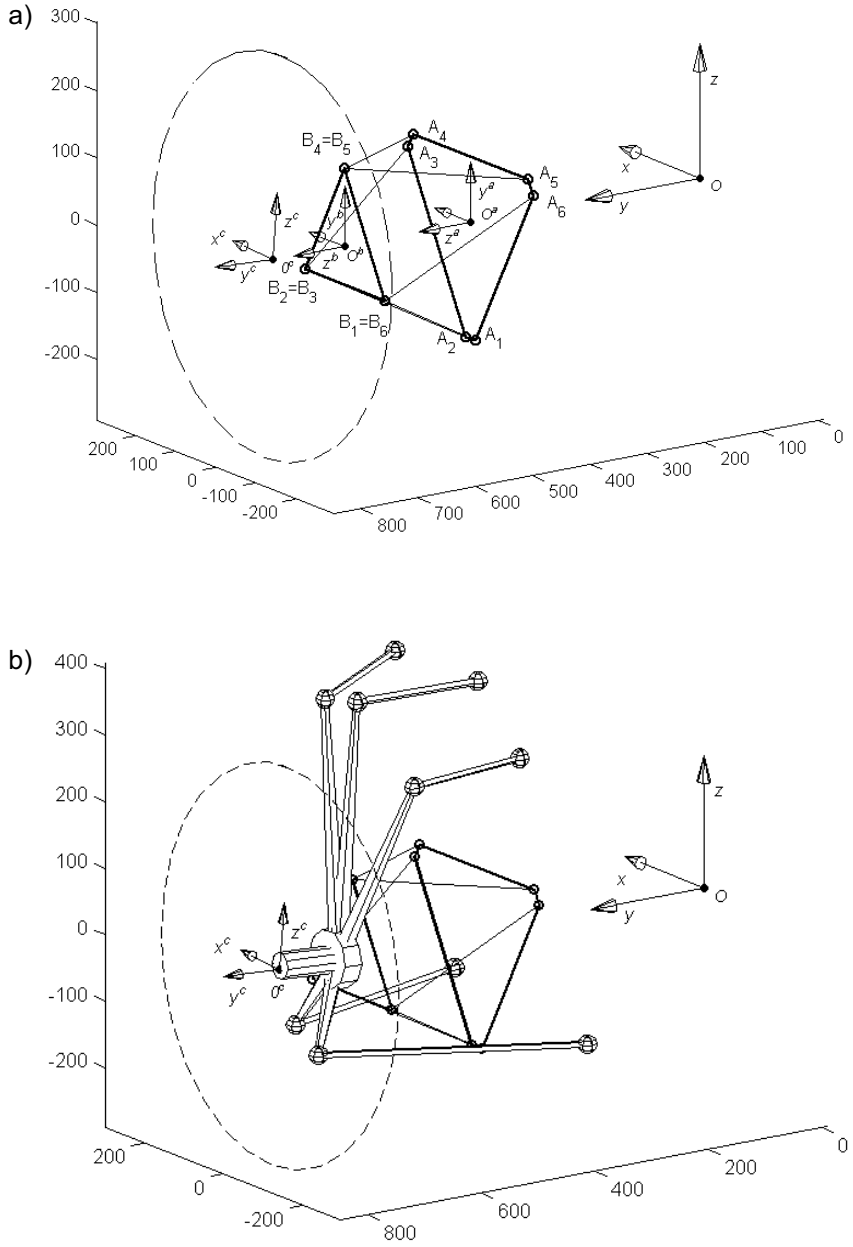

Fig. 6. a) Configuration of the wire mechanism for measuring of the wheel carrier displacement. b) Perspective view of the measuring mechanism with the wheel guiding mechanism in the design position ($p = 0$)

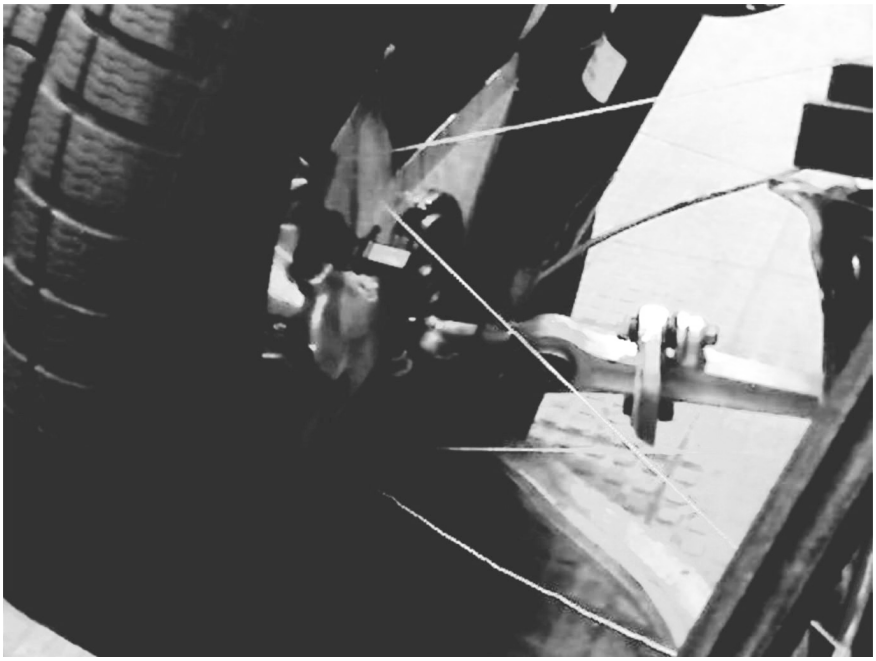

Fig. 7. Configuration of the wire mechanism installed in the actual suspension mechanism of the front wheel in the design position (the wheel carrier is shown from the chassis side)

According to the procedure presented in Fig. 3, the obtained displacement characteristics are presented in Fig. 8. These characteristics are described as the position and orientation coordinates of the measuring platform with respect to the base frame $\{Oxyz\}$. The detailed results of the direct position problem for selected p positions of the platform are presented in Table 3.

The graphical illustrations for the solutions of the direct position problem of the cable mechanism obtained for the successive steps of motion according to changes of the cable lengths l_3 and l_5 are presented in Figs. 9, 10, and 11. The successive positions of the platform frame and the trajectory of the frame origin are presented in Fig. 12.

The measurement results of the cable lengths are used as input data in the computer procedure for solving the direct position problem of the cable mechanism. The obtained solutions are used to determine the position and orientation coordinates of platform B. The conditions for the collision-free trajectory are verified in any point by using the algorithm presented in Fig. 5 in the form of block scheme. Computer programs are implemented in Matlab [12]. The distances (h_{ij}) between the cables are calculated for the given displacements in the range $p \in [0, 95]$ and presented as the characteristics in Fig. 13.

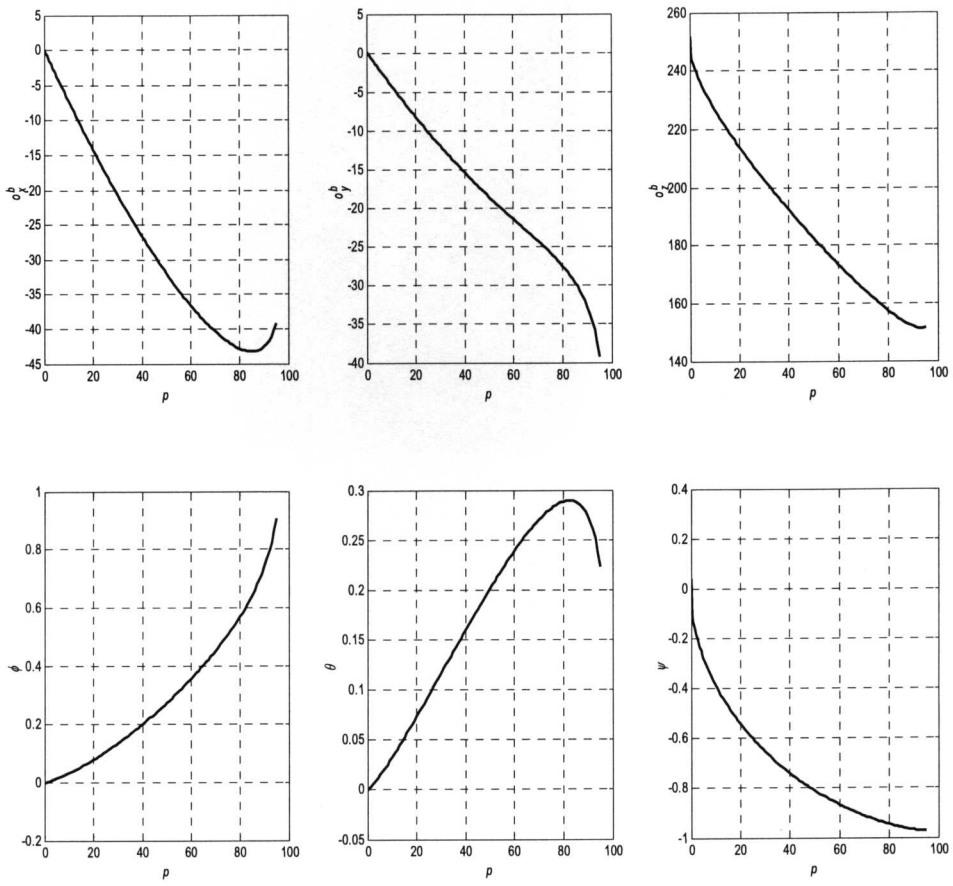

Fig. 8. Position and orientation coordinates of platform B with respect to variable p obtained as solution of the direct position problem for input data given in Table 3

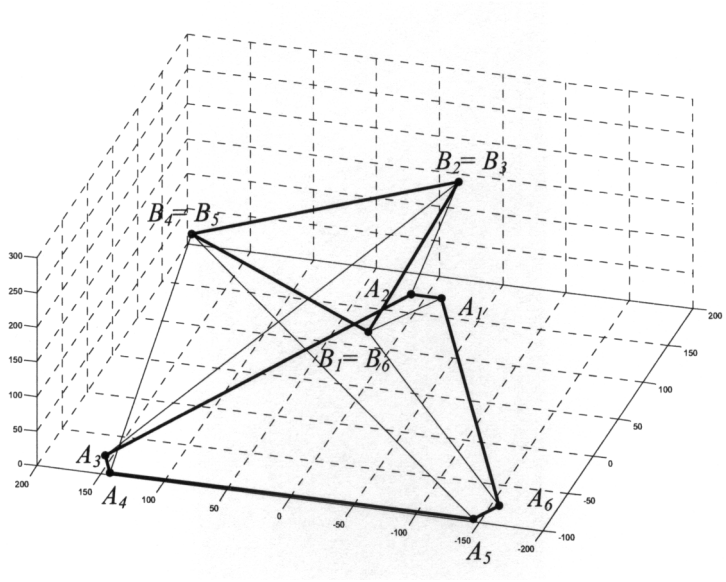

Fig. 9. Cable mechanism presented in position described by $p = 0$ according to Table 4

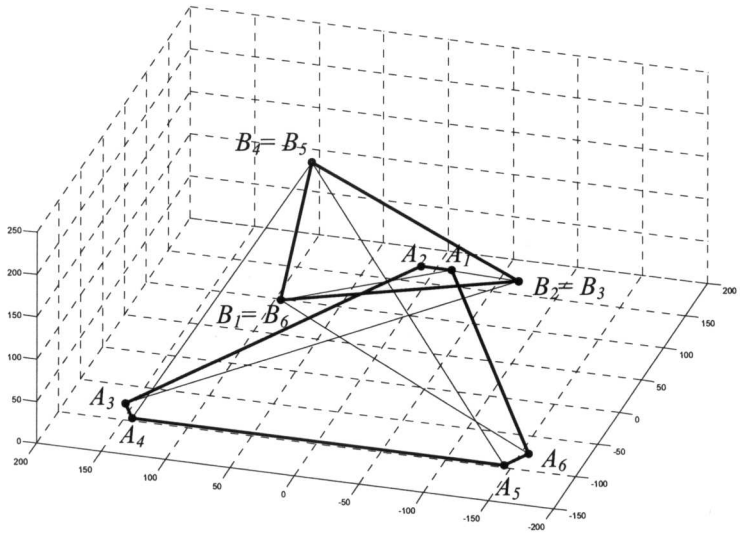

Fig. 10. Cable mechanism presented in position described by $p = 46$ according to Table 4

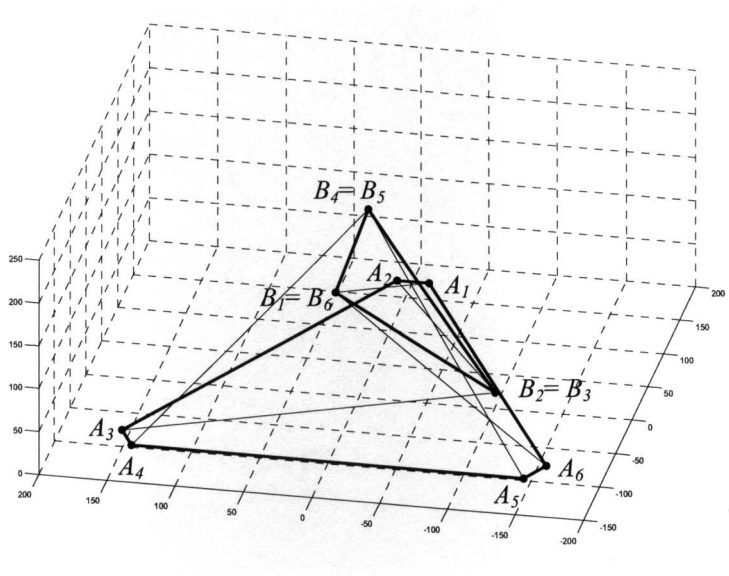

Fig. 11. Cable mechanism presented in position described by $p = 95$ according to Table 4

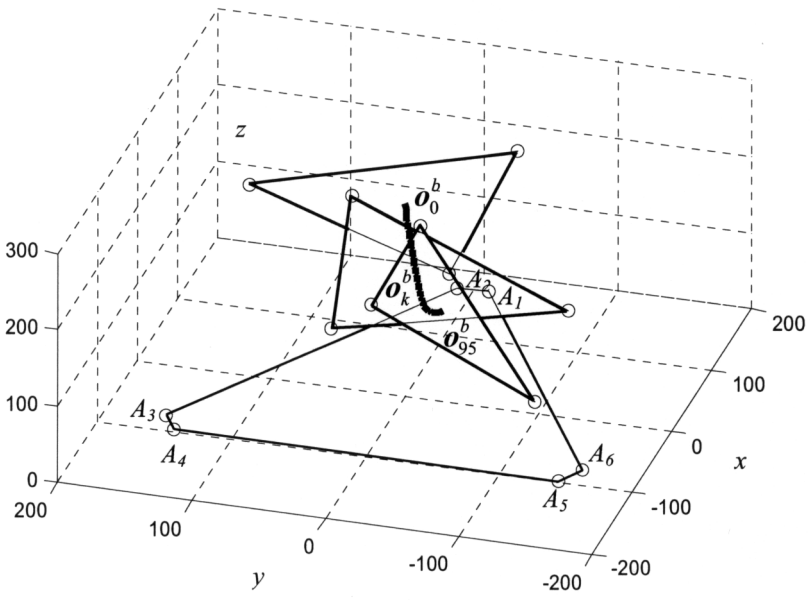

Fig. 12. Successive platform positions for cable mechanism described by $p = 0, 46, 95$, and trajectory of the frame origin $\boldsymbol{o}^b$ for $(p \in [0, 95])$

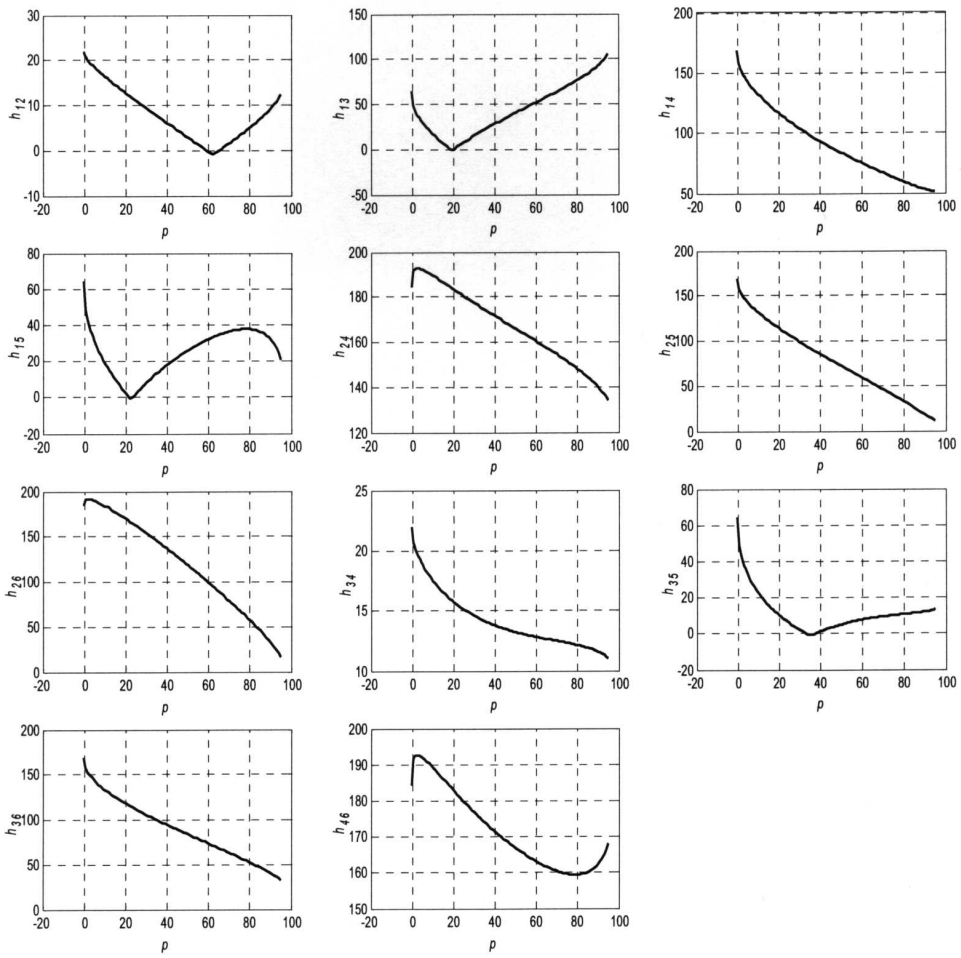

Fig. 13. The distances (h_{ij}) between the cables determined for the considered trajectory of platform B

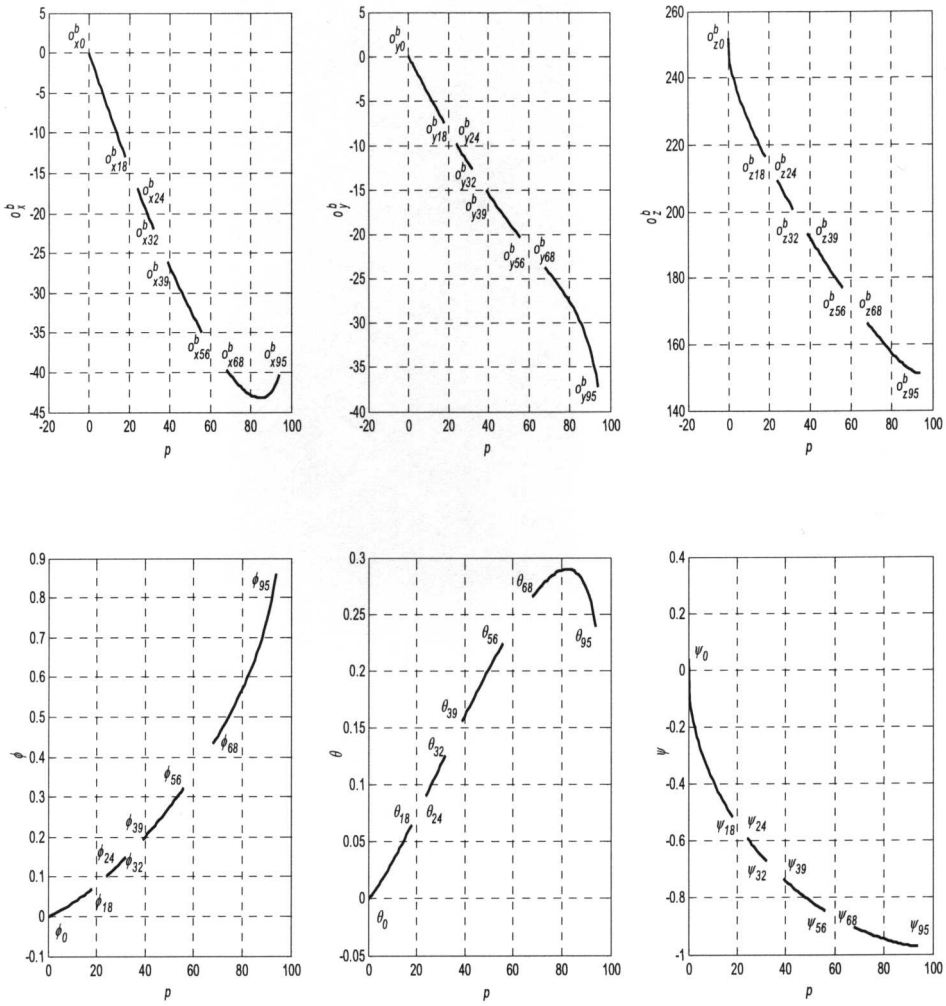

Fig. 14. Position and orientation coordinates of the platform B calculated for given p positions with parts excluded due to cable collisions

In the mechanism pose where the distance between the cables is negative ($h_{ij} < 0$) the collision of the measuring cables takes place. The position coordinates of the cable intersection points Q_i and Q_j obtained from equation (18) for the parameters s_m and t_k are collected in Table 5. The verification of the collision-free conditions can be used to exclude these parts of the platform trajectory, where the platform displacement cannot be measured. According to the procedure presented in Fig. 3, the direct position problem was solved and the free-collision workspace was analyzed (see Fig. 5). The kinematic characteristics described as the position and orientation coordinates of the measuring platform with respect to the base frame $\{Oxyz\}$ are presented in Fig. 14, the parts of the respective curves where the cable collisions take place are excluded.

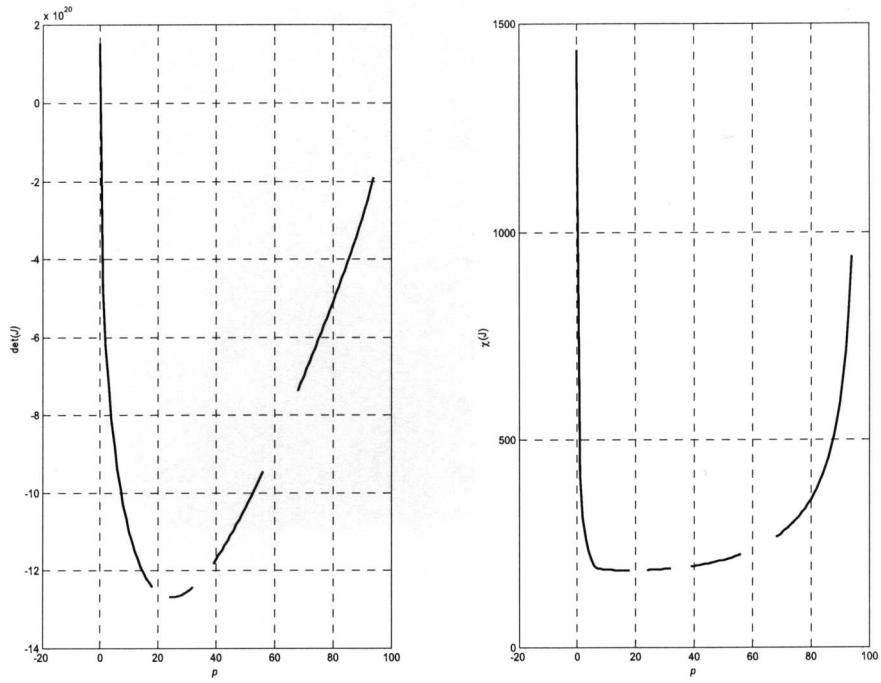

Fig. 15. a) Determinant $det(J)$ and b) condition number of Jacobian matrix calculated for p changes of cable lengths from the range (0, 95), input data are assumed as in example presented in Table 3

The results for the direct problem obtained for p initial and final positions of the platform B are given in Table 6.

In order to verify the singularity conditions for the mechanism trajectory the determinant of Jacobian matrix ($det(\boldsymbol{J})$) and the matrix condition number ($\chi(\boldsymbol{J})$) are calculated as functions of variable p (Fig. 15). The mechanism

positions determined for $p \cong 0$ and $p \cong 95$ are close to singular position, because $det(\boldsymbol{J}) \to 0$, and $\chi(\boldsymbol{J}) \to \infty$. The useful part of the trajectory belongs to the range of $p \in <5, 90>$, where the condition number of the Jacobian matrix is small enough [2] to ensure that the solution procedure for the direct position problem is effective and the accuracy of numerical estimation for the position and orientation of the end-effector is satisfied.

6. Conclusions

The measurement system, presented in this paper, can be used to determine the position and orientation of the end-effector [3] as a solution of the direct position problem formulated for the mechanism with platform of six DOF by using the wire lengths and the coordinates of respective platform points.

This measuring system demonstrates the following properties:

- simple, reliable (without clearances), cheap and light construction,
- high accuracy of the measurement, close to the sensors accuracy, due to the parallel structure of the system,
- possibility of measuring in dynamic condition,
- possibility of improving measurement conditions by suitable selection of the platform positions and the platform points where the wire sensors are fixed,
- possibility of assembling the measuring mechanism in limited workspace, i.e. of the car suspension,
- possibility of using the redundant measurements (with more than six sensors) in order to obtain the smaller bounds of the estimation errors.

The workspace of the considered system is limited by the cable collision-free conditions and singularity-free conditions. The parts of the platform trajectory where the displacement cannot be realized because of the cable collisions are excluded. The proposed algorithm can be used to plan the measurements of real mechanisms, e.g. the ranges of mechanism displacements and cable configurations.

This work was financially supported by Ministry of Science and Higher Education in Poland (Project No N502 059 031/2391).

Appendices

Table 3a.

Coordinates of platform points ($\boldsymbol{a}_i^a$, $\boldsymbol{b}_i^b$, $i = 1, 2...n$, $n \geq 6$)

[mm]	$\boldsymbol{b}_1^b = \boldsymbol{b}_6^b$	$\boldsymbol{b}_2^b = \boldsymbol{b}_3^b$	$\boldsymbol{b}_4^b = \boldsymbol{b}_5^b$	$\boldsymbol{a}_1^a$	$\boldsymbol{a}_2^a$	$\boldsymbol{a}_3^a$	$\boldsymbol{a}_4^a$	$\boldsymbol{a}_5^a$	$\boldsymbol{a}_6^a$
X	−100.0	100.0	0.0	173.2	173.2	−76.2	−96.9	−96.9	−76.2
Y	−57.7	−57.7	115.5	−12.0	12.0	156.0	144.0	−144.0	−156.0
Z	0	0	0	0	0	0	0	0	0

Table 3b.

Lengths of measuring cable

I	1	2	3	4	5	6
l_i [mm]	373.0	269.7	var	269.6	var	269.7
$l_3 = l_5 = 373.0 - p$; $p = 0, 1, ...95$ [mm]						

Table 4.

Position and orientation coordinates of platform B of the measuring mechanism determined for three poses p resulted from changes of cable lengths $l_3 = l_5 = \text{var}$

p [mm]	95	46	0
l_i [mm]	[373.0 269.7 278.0 269.6 278.0 269.7]	[373.0 269.7 324.0 269.6 324.0 269.7]	[373.0 269.7 373.0 269.6 373.0 269.7]
$\boldsymbol{b}_1$	$[-126.2 \quad -12.0 \quad 222.5]^T$	$[-141.3 \quad 14.1 \quad 198.9]^T$	$[-96.7 \quad -63.0 \quad 252.3]^T$
$\boldsymbol{b}_2$	$[-56.5 \quad -113.6 \quad 65.0]^T$	$[-7.4 \quad -124.8 \quad 146.2]^T$	$[103.0 \quad -52.1 \quad 252.4]^T$
$\boldsymbol{b}_3$	$[-56.5 \quad -113.6 \quad 65.0]^T$	$[-7.4 \quad -124.8 \quad 146.2]^T$	$[103.0 \quad -52.1 \quad 252.4]^T$
$\boldsymbol{b}_4$	$[65.0 \quad 8.0 \quad 167.3]^T$	$[54.2 \quad 56.1 \quad 205.2]^T$	$[-6.3 \quad 115.4 \quad 252.3]^T$
$\boldsymbol{b}_5$	$[65.0 \quad 8.0 \quad 167.3]^T$	$[54.2 \quad 56.1 \quad 205.2]^T$	$[-6.3 \quad 115.4 \quad 252.3]^T$
$\boldsymbol{b}_6$ [mm]	$[-126.2 \quad -12.0 \quad 222.5]^T$	$[-141.3 \quad 14.1 \quad 198.9]^T$	$[-96.7 \quad -63.0 \quad 252.3]^T$
$\boldsymbol{o}^b$ [mm]	$[-39.2 \quad -39.2 \quad 151.6]^T$	$[-31.5 \quad -18.2 \quad 183.5]^T$	$[0.0 \quad 0.1 \quad 247.5]^T$
$[\varphi, \theta, \psi]$ [rad]	$[0.9 \quad 0.2 \quad -1.0]^T$	$[0.3 \quad 0.2 \quad -0.8]^T$	$[0.0 \quad 0.0 \quad -0.1]^T$
$\boldsymbol{R}^b$	$\begin{bmatrix} 0.3487 & 0.9026 & 0.2525 \\ -0.5082 & 0.4084 & -0.7583 \\ -0.7875 & 0.1361 & 0.6011 \end{bmatrix}$	$\begin{bmatrix} 0.6692 & 0.7421 & 0.0381 \\ -0.6949 & 0.6432 & -0.3217 \\ -0.2633 & 0.1888 & 0.9461 \end{bmatrix}$	$\begin{bmatrix} 0.9985 & 0.0544 & -0.0002 \\ -0.0544 & 0.9985 & -0.0004 \\ 0.0002 & -0.0003 & 1.0000 \end{bmatrix}$

Table 5.
Position coordinates of intersection points between the measuring wires determined for the considered trajectory of platform B

$h_{ij} < 0$ [mm]	i	j	p [mm]	t_k	s_m	$\boldsymbol{q}_i$ [mm]	$\boldsymbol{q}_j$ [mm]
	1	2	65 ... 59	0.0961 ... 0.0959	0.1538 ... 0.1538	$[142.8 \quad -9.1 \quad 18.7]^T$ ... $[142.9 \quad -9.2 \quad 18.8]^T$	$[142.3 \quad -9.1 \quad 17.9]^T$ ... $[143.4 \quad -9.2 \quad 19.6]^T$
	1	3	20 19	0.5805 0.5798	0.6235 0.6243	$[-2.6 \quad -8.5 \quad 126.4]^T$ $[-2.0 \quad -9.2 \quad 126.7]^T$	$[-3.0 \quad -9.0 \quad 125.8]^T$ $[-1.6 \quad -8.6 \quad 127.2]^T$
	1	5	23 22	0.6064 0.6077	0.5939 0.5924	$[-11.5 \quad -6.5 \quad 130.4]^T$ $[-11.6 \quad -7.1 \quad 131.2]^T$	$[-11.2 \quad -7.1 \quad 130.9]^T$ $[-11.7 \quad -6.7 \quad 130.9]^T$
	3	5	37 ... 34	0.6710 ... 0.6607	0.5335 ... 0.5429	$[-18.0 \quad -29.9 \quad 113.5]^T$ ... $[-15.6 \quad -26.1 \quad 115.6]^T$	$[-17.3 \quad -29.9 \quad 113.1]^T$ ... $[-16.3 \quad -26.0 \quad 116.0]^T$

Table 6.
Position and orientation coordinates of platform B of the measuring mechanism determined for initial and final p poses of a given platform trajectory

a)

p [mm]	68	56	39
l_i [mm]	[373.0 269.7 305.0 269.6 305.0 269.7]	[373.0 269.7 317.0 269.6 317.0 269.7]	[373.0 269.7 334.0 269.6 334.0 269.7]
$\boldsymbol{b}_1$	$[-143.6 \quad 18.2 \quad 194.6]^T$	$[-142.6 \quad 16.5 \quad 196.4]^T$	$[-138.5 \quad 9.3 \quad 203.8]^T$
$\boldsymbol{b}_2$	$[-31.2 \quad -124.5 \quad 110.9]^T$	$[-16.9 \quad -125.5 \quad 133.1]^T$	$[7.4 \quad -121.9 \quad 165.3]^T$
$\boldsymbol{b}_3$	$[-31.2 \quad -124.5 \quad 110.9]^T$	$[-16.9 \quad -125.5 \quad 133.1]^T$	$[7.4 \quad -121.9 \quad 165.3]^T$
$\boldsymbol{b}_4$	$[55.7 \quad 35.3 \quad 193.9]^T$	$[54.8 \quad 48.3 \quad 201.3]^T$	$[52.7 \quad 67.5 \quad 210.8]^T$
$\boldsymbol{b}_5$	$[55.7 \quad 35.3 \quad 193.9]^T$	$[54.8 \quad 48.3 \quad 201.3]^T$	$[52.7 \quad 67.5 \quad 210.8]^T$
$\boldsymbol{b}_6$ [mm]	$[-143.6 \quad 18.2 \quad 194.6]^T$	$[-142.6 \quad 16.5 \quad 196.4]^T$	$[-138.5 \quad 9.3 \quad 203.8]^T$
$\boldsymbol{o}^b$ [mm]	$[-39.7 \quad -23.7 \quad 166.5]^T$	$[-34.9 \quad -20.3 \quad 176.9]^T$	$[-26.1 \quad -15.0 \quad 193.3]^T$
$[\varphi, \theta, \psi]$ [rad]	$[0.4 \quad 0.3 \quad -0.9]^T$	$[0.3 \quad 0.2 \quad -0.8]^T$	$[0.2 \quad 0.2 \quad -0.7]^T$
$\boldsymbol{R}^b$	$\begin{bmatrix} 0.5618 & 0.8261 & 0.0441 \\ -0.7136 & 0.5109 & -0.4793 \\ -0.4185 & 0.2378 & 0.8765 \end{bmatrix}$	$\begin{bmatrix} 0.6288 & 0.7766 & 0.0380 \\ -0.7101 & 0.5935 & -0.3788 \\ -0.3168 & 0.2112 & 0.9247 \end{bmatrix}$	$\begin{bmatrix} 0.7296 & 0.6828 & 0.0379 \\ -0.6562 & 0.7146 & -0.2421 \\ -0.1924 & 0.1518 & 0.9695 \end{bmatrix}$

b)

p [mm]	32	24	18
l_i [mm]	[373.0 269.7 341.0 269.6 341.0 269.7]	[373.0 269.7 349.0 269.6 349.0 269.7]	[373.0 269.7 355.0 269.6 355.0 269.7]
$\boldsymbol{b}_1$	$[-135.9 \quad 4.8 \quad 208.2]^T$	$[-132.0 \quad -1.9 \quad 214.2]^T$	$[-128.3 \quad -8.3 \quad 219.6]^T$
$\boldsymbol{b}_2$	$[19.0 \quad -118.4 \quad 178.7]^T$	$[33.4 \quad -112.5 \quad 194.1]^T$	$[45.3 \quad -106.6 \quad 205.7]^T$
$\boldsymbol{b}_3$	$[19.0 \quad -118.4 \quad 178.7]^T$	$[33.4 \quad -112.5 \quad 194.1]^T$	$[45.3 \quad -106.6 \quad 205.7]^T$
$\boldsymbol{b}_4$	$[51.0 \quad 75.7 \quad 214.8]^T$	$[47.9 \quad 85.3 \quad 219.7]^T$	$[44.3 \quad 92.6 \quad 223.8]^T$
$\boldsymbol{b}_5$	$[51.0 \quad 75.7 \quad 214.8]^T$	$[47.9 \quad 85.3 \quad 219.7]^T$	$[44.3 \quad 92.6 \quad 223.8]^T$
$\boldsymbol{b}_6$ [mm]	$[-135.9 \quad 4.8 \quad 208.2]^T$	$[-132.0 \quad -1.9 \quad 214.2]^T$	$[-128.3 \quad -8.3 \quad 219.6]^T$
$\boldsymbol{o}^b$ [mm]	$[-22.0 \quad -12.6 \quad 200.6]^T$	$[-16.9 \quad -9.7 \quad 209.3]^T$	$[-12.9 \quad -7.4 \quad 216.4]^T$
$[\varphi, \theta, \psi]$ [rad]	$[0.1 \quad 0.1 \quad -0.7]^T$	$[0.1 \quad 0.1 \quad -0.6]^T$	$[0.1 \quad 0.1 \quad -0.5]^T$
$\boldsymbol{R}^b$	$\begin{bmatrix} 0.7740 & 0.6321 & 0.0367 \\ -0.6158 & 0.7650 & -0.1886 \\ -0.1473 & 0.1234 & 0.9814 \end{bmatrix}$	$\begin{bmatrix} 0.8269 & 0.5614 & 0.0328 \\ -0.5533 & 0.8227 & -0.1306 \\ -0.1003 & 0.0898 & 0.9909 \end{bmatrix}$	$\begin{bmatrix} 0.8682 & 0.4954 & 0.0281 \\ -0.4914 & 0.8662 & -0.0905 \\ -0.0692 & 0.0647 & 0.9955 \end{bmatrix}$

Manuscript received by Editorial Board, March 16, 2007;
final version, October 26, 2007.

REFERENCES

[1] Grandon C., et al.: Certified Pose determination under Uncertainties. Proc. of the 12th IFToMM World Congress, Besancon 2006.

[2] Góra M., Knapczyk J., Maniowski M.: Analiza położeń i przemieszczeń mechanizmu przestrzennego przy wykorzystaniu pomiarów czujnikami linkowymi. XX Konferencja Naukowo-Dydaktyczna TMM, Zielona Góra, 2006.

[3] Góra M., Knapczyk J., Maniowski M.: Zmiany orientacji koła względem jezdni wywołane przechyłem nadwozia samochodu. Teka Komisji Nauk.-Probl. Motoryzacji, PAN O/Kraków, Kraków 2005.

[4] Góra M., Knapczyk J.: Analiza przemieszczeń mechanizmu wielowahaczowego prowadzącego zwrotnicę koła samochodu osobowego. Wydawnictwo Instytutu Technologii i Eksploatacji (XIX Konf. Nauk.-Dyd. TMM Kraków), Radom 2004.

[5] Góra M., Knapczyk J.: Analiza przemieszczeń modelu stawu kolanowego o ruchu przestrzennym. Przegląd lekarski 61/2004, str. 65-67.

[6] Jeong J. W., Kim S. H., Kwak Y. K.: Kinematics and workspace analysis of a parallel wire mechanism for measuring a robot pose. Mechanism and Machine Theory, vol. 34 (1999), pp. 825÷841.

[7] Knapczyk J., Maniowski M.: Dimensional synthesis of a five-rod guiding mechanism for car front wheels. The Archive of Mechanical Engineering, vol. 50, Nr 1, 2003.
[8] Merlet J. P.: Jacobian, Manipulability, Condition Number, and Accuracy of Parallel Robots. Trans. ASME, Journal of Mechanical Design, January 2006, vol. 128.
[9] Morecki A., Knapczyk J., Kędzior K.: Teoria mechanizmów i manipulatorów, WNT Warszawa, 2002.
[10] Verhoeven R., Hiller M., Tadokoro S.: Workspace, stiffness, singularities and classification of tendon-driven Stewart platforms. Advances in Robot Kinematics: Analysis and Control. Kluwer Academic Publ. 1998.
[11] Kaczorek T.: Wektory I macierze w automatyce i elektrotechnice. WNT, Warszawa, 1998.
[12] Brzózka J., Dorobczyński L.: Programowanie w Matlab. Wyd. MIKOM, Warszawa, 1998.

Estymacja przestrzennego położenia i przemieszczenia platformy mechanizmu o strukturze równoległej na podstawie pomiarów czujnikami linkowymi

S t r e s z c z e n i e

W artykule przedstawiono metodę estymacji parametrów przestrzennego położenia i przemieszczenia mechanizmu wielo-wahaczowego zawieszenia koła samochodu na podstawie wyników pomiarów za pomocą czujników linkowych. Pewne zmiany pozycji i orientacji platformy zamocowanej do zwrotnicy koła powodują odpowiednie zmiany długości linek czujników. Punkty zaczepienia czujników linkowych dobrano uwzględniając warunki uniknięcia kolizji. Przykład liczbowy dotyczy analizy położeń i przemieszczeń platformy oraz usytuowania czujników dające dobre uwarunkowania pomiarów.